Bioorganic Chemistry 109 (2021) 104736

Contents lists available at ScienceDirect

Bioorganic Chemistry

journal homepage: www.elsevier.com/locate/bioorg

Design, synthesis and biological evaluations of diverse Michael acceptor-based phenazine hybrid molecules as TrxR1 inhibitors

Yucheng Zhong [a,b,1], Jing Liu [c,1], Xiangyu Cheng [c], Hao Zhang [c], Chunhua Zhang [c], Zhuolu Xia [c], Zhongxi Wu [c], Lu Zhang [c], Yuting Zheng [c], Zhanyu Gao [c], Zhidong Jiang [c], Zhixiang Wang [a,c], Dechun Huang [a,c], Yuanyuan Lu [a,b,*], Feng Jiang [a,c,*]

[a] State Key Laboratory of Natural Medicines, China Pharmaceutical University, Nanjing 210009, China
[b] School of Life Science and Technology, China Pharmaceutical University, Nanjing 210009, China
[c] School of Engineering, China Pharmaceutical University, Nanjing 210009, China

ARTICLE INFO

Keywords:
Phenazines
Michael receptor
Antiproliferative activity
TrxR1 inhibitor

ABSTRACT

A series of novel phenazine derivatives (**1**~**27**) containing the Michael acceptor scaffolds were designed and synthesized in this study. Some compounds exhibited selective cytotoxicity against Bel-7402 cancer cell line *in vitro*, in which compound **26** were found to have the best antiproliferative activity. Meanwhile, compound **26** showed no obvious cell toxicity against human normal liver epithelial L02 cells, which means this compound possessed a better safety potential. In the following research, compound **26** was verified to inhibit TrxR1 enzyme activity, ultimately resulting in cellular molecular mechanism events of apoptosis including growth of intracellular ROS level, depletion of reduced Trx1, liberation of ASK1 and up-regulation of p38, respectively. Together, all these evidences implicated that compound **26** acted as the TrxR1 inhibitor against Bel-7402 cells, and could activate apoptosis through the ROS-Trx-ASK1-p38 pathway.

1. Introduction

Phenazines, a large group of natural or synthetic nitrogen-containing heterocyclic compounds, have been reported to be associated with anticancer activities since 1959. Phenazine compounds are a kind of secondary metabolites of microorganisms with redox activity [1]. The mammalian Thioredoxin reductase (TrxR) proteins, existing mainly as the cytosolic TrxR1 and mitochondrial TrxR2, are seleno-flavoenzymes containing a penultimate C-terminal selenocysteine (*Sec*) residue, and it is a NADPH-dependent dimer selenoenzyme containing Flavin Adenine Dinucleotide (FAD) domain, belonging to pyridine nucleotide-disulfide oxidoreductase family members [2]. TrxR1 has also been found to be overexpressed in a variety of cancer cells [3]. TrxR1 is necessary to convert Trx1 from the oxidized states to the reduced forms, improving the viability of cells under oxidative stress [4], which is especially important for cancer cells with high redox levels. The abnormal function of TrxR/Trx enzyme is related to a variety of pathological conditions, including cancer, inflammation and neurodegenerative diseases [5].

In previous study [6], we have discovered a natural phenazine derivative *N*-(2-hydroxyphenyl)-2-phenazinamine (**A**) (Fig. 1), isolated from a marine actinomycete BM-17, which showed high cytotoxicity against several cancer cells. Subsequently we synthesized a series of 2-phenazinamine derivatives, in which compound **B** (Fig. 1) was found to possess good cytotoxic activities against K562 and HepG2 cancer cells [7]. Furthermore, based on the molecular hybridization strategy, we designed, synthesized and screened several phenazine hybrid molecules as antitumor agents such as **C** [8], **D** [9], **E** [10] and **F** [11] (Fig. 1). Among of them, compound **D** was found to show the most potential than positive control drug against HepG2 cancer cells both *in vivo* and *in vitro* [9]. Moreover, our previous studies have proven that the phenazine hybrid molecule **D** played the significant role in anti-tumor activities through inhibiting TrxR1 pathway [12].

A variety of TrxR1 enzyme inhibitors have been reported to selectively inhibit the growth of cancer cells [3,13–15]. Recently, Fang et al [16], synthesized a series of Michael acceptor-based 1,4-naphthoquinone derivatives and discovered compound **G** (Fig. 1) as a potent cytotoxic agent with a submicromolar half maximal inhibitory concentration to HL-60 cells. The cellular action of compound **G** is related to its ability

* Corresponding authors.
E-mail addresses: luyy@cpu.edu.cn (Y. Lu), jiangfeng@cpu.edu.cn (F. Jiang).
[1] Y.Z. and J.L. contributed equally to this work.

https://doi.org/10.1016/j.bioorg.2021.104736
Received 22 December 2020; Received in revised form 23 January 2021; Accepted 4 February 2021
Available online 19 February 2021

to target the selenoenzyme TrxR. It could induce ROS production and promote oxidative stress-mediated apoptosis in HL-60 cells. Michael acceptor-based scaffolds have been widely used as an effective template in medicinal chemistry for drug discovery. Michael acceptors (i.e., alkenes attached to electron-withdrawing groups such as ester, carbonyl, cyano, nitro and sulfonyl group) containing an electrophile are generally biologically active, which were involved in the regulation of many signaling pathways in cells. Chalcone, a potential Michael acceptor, containing an α,β-unsaturated carbonyl scaffold, can readily form covalent bonds with the sulfhydryl of cysteine or other thiols to obtain the Michael adducts, which may play an important role in the biological activities [17]. When combining Michael acceptor-based scaffolds and natural compound skeletons to produce novel hybrid molecules, it will greatly increase the probability of discovering new drug leads with clinical potentials against various diseases [18–20].

The above results inspired us that the phenazine derivative **D** inhibited TrxR1 mainly through combining to *Sec* residues of TrxR1, which was further evidenced by docking results between **D** and TrxR1 [12]. To continue the investigation of phenazine analogues as potential TrxR1 inhibitors, in the present study, we synthesized a series of novel phenazine derivatives which were designed as hybrid molecules of phenazine and Michael acceptor-based scaffolds. Here, we reported the facile construction of a structurally diverse compound library for a better investigation of the antitumor activity, TrxR1 inhibitory activity and mechanism of action of these novel compounds.

2. Results and discussion

2.1. Chemistry

According to the procedure described in the literatures, we synthesized a series of important phenazine precursors including 1-methoxyphenazine [21], 2-amino-3-hydroxyphenazine [22], 2,3-dihydroxyphenazine [23], 1-aminophenazine [24], 2-aminophenazine [7] and 2,3-diaminophenazine [22]. After treated with BBr_3, 1-methoxyphenazine was transformed to 1-hydroxyphenazine, which subsequently reacted with diverse acryloyl chlorides to get compounds **1~4** (Scheme 1). Similarly, 2-amino-3-hydroxyphenazine, 2,3-dihydroxyphenazine, 1-aminophenazine, 2-aminophenazine and 2,3-diaminophenazine reacted with diverse acryloyl chlorides to get compounds **5~23**, respectively, as shown in Schemes 2–6. Furthermore, we used 1,4-phenylenediamine as the starting material to synthesize 6-methoxy-2-aminophenazine following the modified method in the literature [21], which subsequently reacted with diverse acryloyl chlorides to get compounds **24~27** (see Scheme 7).

2.2. Cell proliferation and TrxR1 inhibitory activities of compounds 1~27

MTT assay was applied to preliminarily screen the synthesized phenazine compounds in which several compounds with strong cytotoxicity against cancer cells were detected. By comparing the cytotoxicity of different compounds on various cells including five kinds of cancer cell lines and one kind of normal liver cell line (Table 1), surprisingly, four compounds **19**, **20, 26** and **27** with certain significances in cytotoxicity were found, which are relatively more specific to liver cancer cells than the other cells. Specifically, compound **19** and **20** displayed good cytotoxicity against HuH-7 cells (IC_{50} = 6.1 and 9.6 μM, respectively) and Bel-7402 cells (IC_{50} = 8.2 and 12.4 μM, respectively). Meanwhile, compound **19** displayed better cytotoxicity against MCF-7 cells. Compound **27** displayed commensurate cytotoxicity than the positive drug Cisplatin. In particular, compared with Cisplatin, compound **26** displayed better or commensurate cytotoxicity against three kinds of liver cancer cells (HepG2, HuH-7 and Bel-7402 cells) rather than human breast cancer cell MCF-7 and human gastric cancer cell SGC-7901, and meanwhile, it displayed lower cytotoxicity against one kind of normal liver cells (L02 cells). Hence, it could be said that compound **26** showed better selectivity and possessed good targeting ability to liver cancer cells.

All compounds were designed as hybrid molecules of α,β-unsaturated carbonyl scaffold and diverse phenazine precursors including 1-hydroxyphenazine, 2-amino-3-hydroxyphenazine, 2,3-dihydroxyphenazine, 1-aminophenazine, 2-aminophenazine and 2,3-diaminophenazine, while comparing the relationship of compounds' structure and cytotoxicity, we could conclude that 2-amino substitution on the phenazine core plays a particularly critical role to improve compounds' cytotoxicity. Furthermore, when the strong electron-withdrawing group including fluoro or trifluoromethyl substituent group was attached to

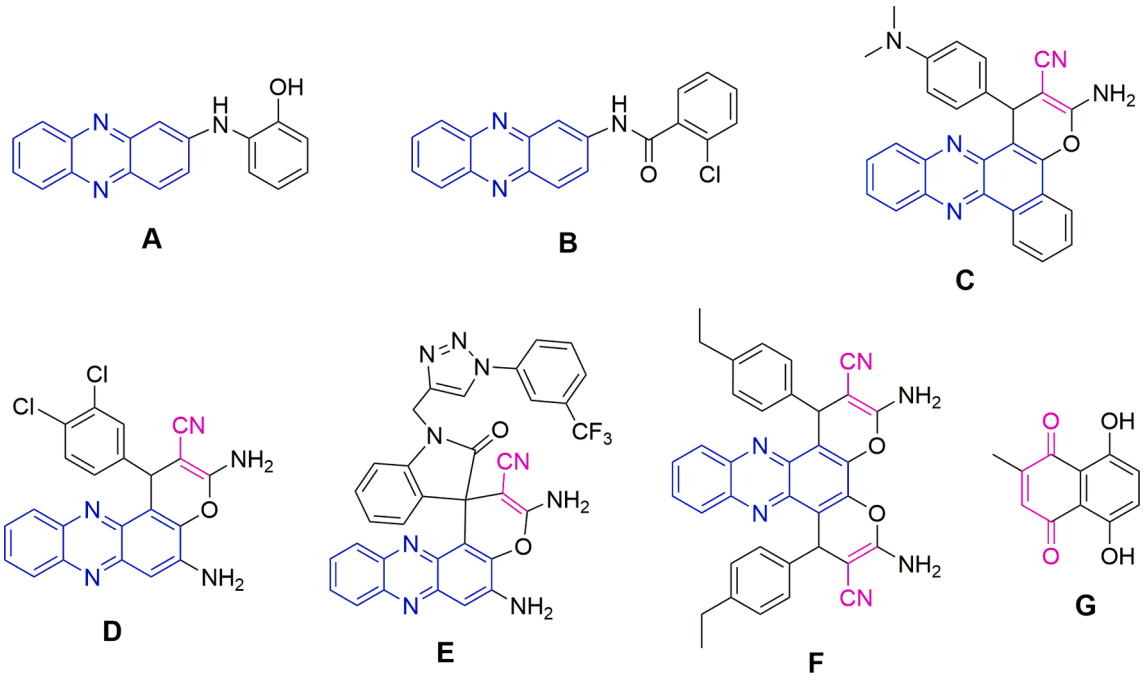

Fig. 1. Structures of compounds **A**-**G**.

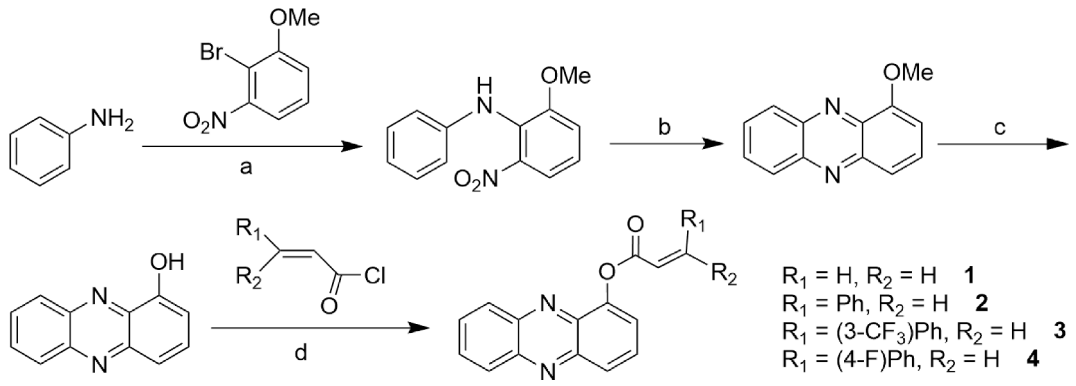

Scheme 1. Synthetic routes of compounds **1**~**4**. Reagents and conditions: (a)$Pd_2(dba)_3$, *rac*-BINAP, NaOtBu, PhMe, 110 °C; (b) $NaBH_4$, NaOtBu, EtOH, 60 °C; (c) BBr_3, DCM; (d) Pyridine, DCM.

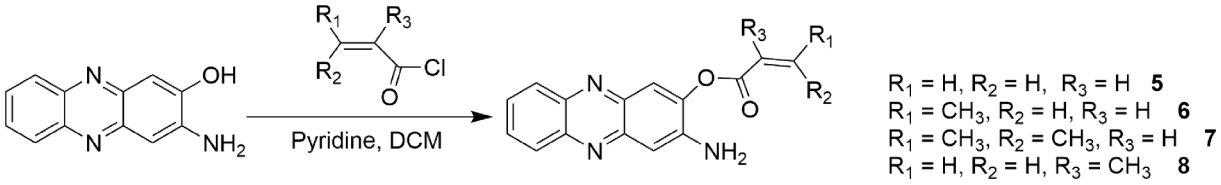

Scheme 2. Synthetic route of compounds **5**~**8**.

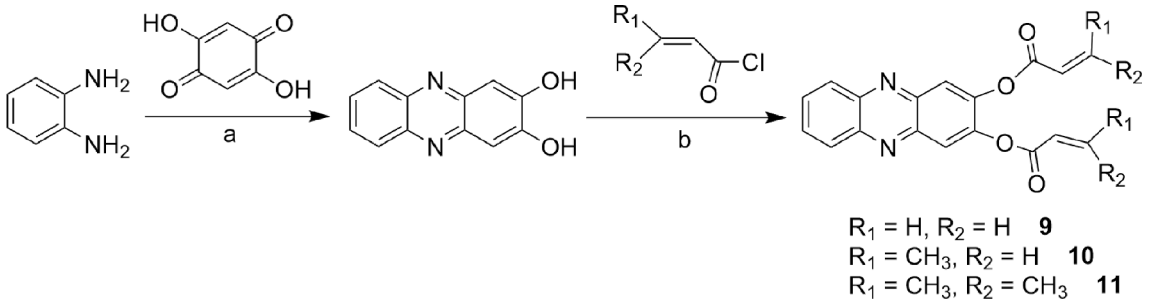

Scheme 3. Synthetic routes of compounds **9**~**11**. Reagents and conditions: (a) H_2O, 100 °C; (b) Pyridine, DCM.

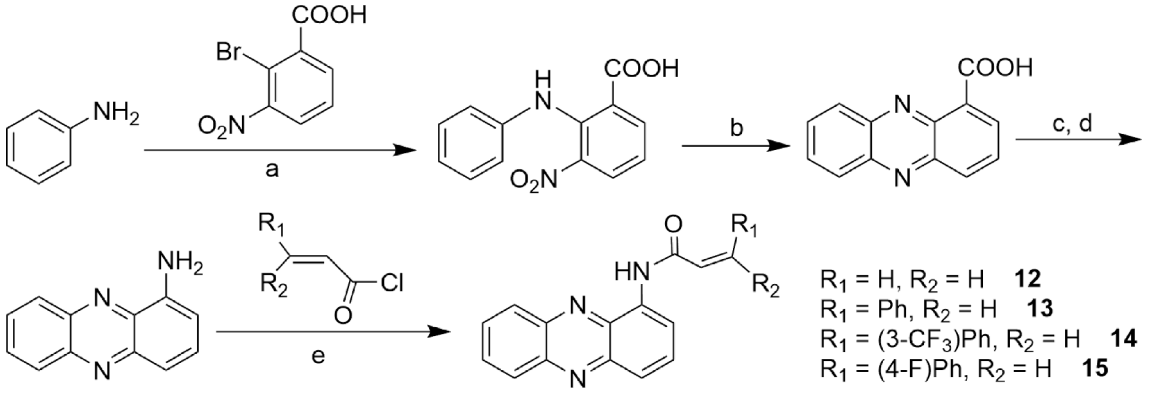

Scheme 4. Synthetic routes of compounds **12**~**15**. Reagents and conditions: (a) Cu powder, CuCl, *N*-ethylmorpholine, 2,3-butanediol; (b) $NaBH_4$, NaOH, H_2O; (c) DPPA, TEA; (d) H_2O; (e) Pyridine, DCM.

α,β-unsaturated carbonyl scaffold, compounds' antiproliferative activity was significantly improved, just like compounds **19**, **20, 26** and **27**.

In addition, the TrxR1 inhibitory activities of related compounds were further evaluated in free cells assays. The results indicated that the compounds' inhibitory activities of TrxR1 were congruously associated with the pace of cytotoxicities. Moreover, compound **26**, one of the best batch of compounds, displayed the best inhibitory level of TrxR1 enzyme activity (EC_{50} = 21.4 μM). Therefore, compound **26** was selected for the follow-up research.

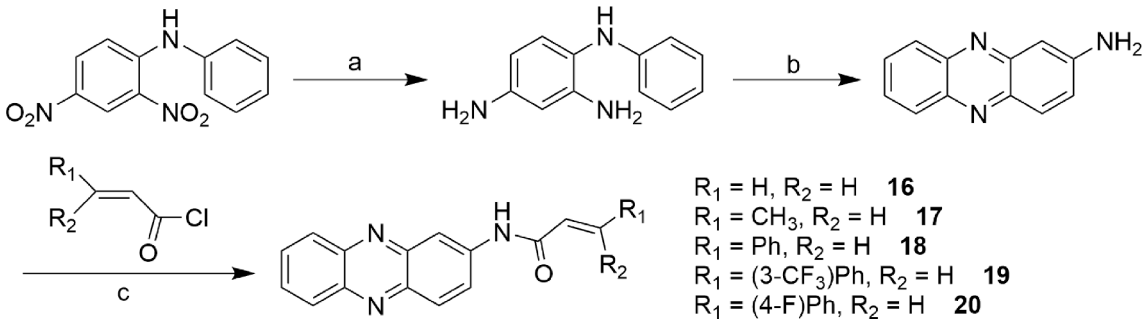

Scheme 5. Synthetic routes of compounds **16**~**20**. Reagents and conditions: (a) Pd/C, H_2; (b) $PhNO_2$, $MgSO_4$; (c) Pyridine, DCM.

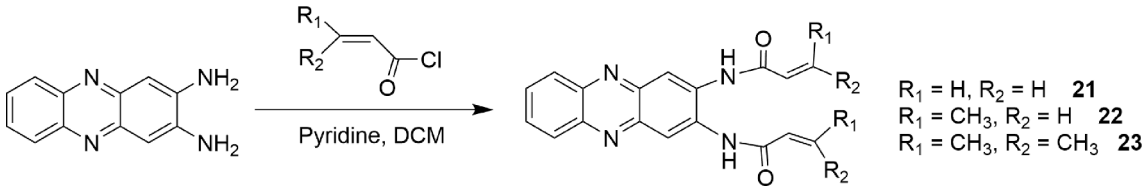

Scheme 6. Synthetic routes of compounds **21**~**23**.

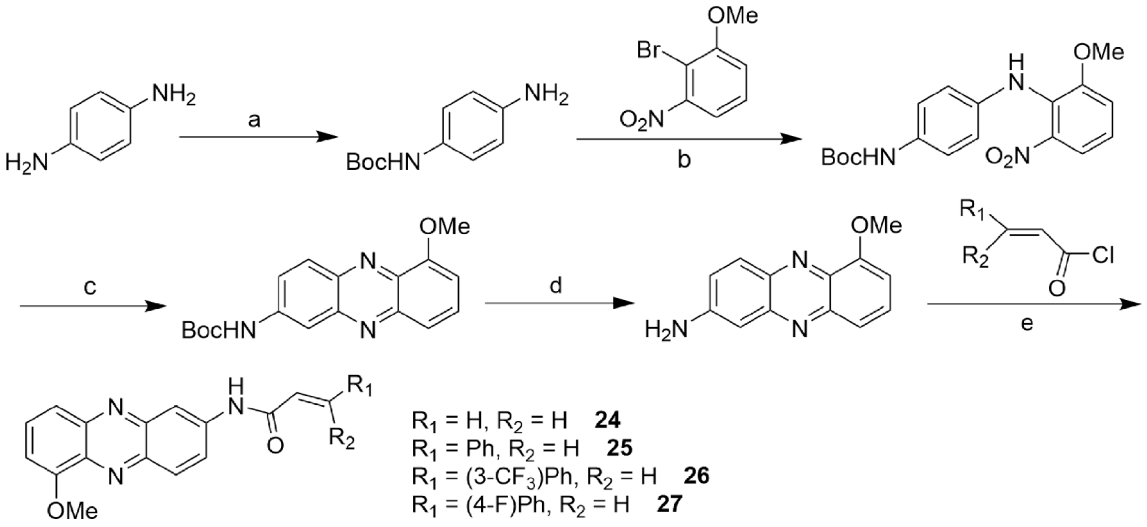

Scheme 7. Synthetic routes of compounds **24**~**27**. Reagents and conditions: (a) $(Boc)_2O$; (b) $Pd_2(dba)_3$, *rac*-BINAP, NaOtBu, PhMe, 110 °C; (c) $NaBH_4$, NaOtBu, EtOH, 60 °C; (d) TFA, DCM; (e) Pyridine, DCM.

*2.3. Compound **26** will increase the level of reactive oxygen species through inhibiting TrxR1 in Bel-7402 cells*

Inhibition of TrxR1 deeply affected the intracellular redox system balance and increased reactive oxygen species (ROS) [25]. And the cellular H_2O_2 level within a certain period of time after administrations were detected for which H_2O_2 is a primary component of cellular ROS [5,26]. After adding compound **26**, the H_2O_2 level increased significantly with time compared to the control group (Fig. 2a).

The following time-course experiments were tested to figure out the relationship between TrxR1, GSH, and H_2O_2. Firstly, non-reductive western blotting was performed on thioredoxin redox status (Fig. 2b). It was found that Trx1 in the reduced state decreased significantly from 0.5 h after the administration, and then increased to a certain extent, but never returned to the previous level. Meanwhile, the Trx1 in the oxidized state showed a trend of increasing with the administration time, and a high level has been maintained after 2 h of administration. The above results showed that compound **26** could affect the redox level of Trx1 in cells by inhibiting TrxR1 enzyme activity. Secondly, the ratio of GSH/GSSG was measured in cells at different time after treated the same doses of compound **26** (Fig. 2c). It was found that at 2 h, the ratio of GSH decreased significantly compared with the control group, and then gradually returned to the original level.

In combination with the above time-course experiments, it could be supposed that the ROS produced by the cancer cells was mainly eliminated by the reduced Trx1, and the H_2O_2 content did not increase sharply in a short period of time. If TrxR1 enzyme activity was inhibited by compound **26**, the ROS could not be eliminated by the oxidized Trx1 and gradually accumulated in the cell [27]. Interestingly, the H_2O_2 content was still increasing after the intracellular reduced glutathione returned to the original level, which indicated that compound **26** will not affect the glutathione system.

Table 1
Six kinds of cells (HepG2, HuH-7, Bel-7402, L02, MCF-7, SGC-7901) were co-cultured with different concentrations of different compounds for 48 h, and then cell viability was determined by MTT method and IC_{50} value was calculated.

No.	IC_{50} values* (μM)						EC_{50}* values (μM)
	HepG2	HuH-7	Bel-7402	L02	MCF-7	SGC-7901	
1	>50	>50	>50	33.0 ± 2.1	39.1 ± 0.6	39.2 ± 1.5	>50
2	35.5 ± 4.2	>50	29.7 ± 0.7	35.1 ± 0.8	25.5 ± 2.6	>50	>50
3	>50	>50	>50	>50	>50	>50	>50
4	31.4 ± 5.7	>50	25.9 ± 1.6	39.1 ± 2.5	26.7 ± 2.0	>50	>50
5	>50	>50	>50	>50	>50	>50	>50
6	>50	>50	>50	>50	>50	>50	>50
7	>50	>50	>50	>50	>50	>50	>50
8	>50	>50	>50	>50	>50	>50	>50
9	>50	>50	>50	>50	>50	>50	>50
10	>50	>50	>50	>50	>50	>50	>50
11	>50	>50	>50	>50	>50	>50	>50
12	>50	>50	26.6 ± 4.8	39.6 ± 1.8	>50	38.4 ± 0.5	>50
13	37.2 ± 5.9	>50	>50	>50	>50	>50	>50
14	>50	>50	>50	>50	>50	>50	>50
15	>50	>50	>50	>50	>50	>50	>50
16	>50	>50	>50	>50	>50	>50	>40
17	>50	>50	>50	>50	>50	>50	>50
18	18.8 ± 2.7	10.7 ± 0.8	16.5 ± 1.5	49.1 ± 4.1	20.9 ± 1.4	20.9 ± 1.1	>50
19	20.6 ± 2.9	6.14 ± 0.36	8.24 ± 0.27	18.6 ± 1.1	9.8 ± 0.7	9.60 ± 0.62	25.0 ± 3.8
20	19.3 ± 3.2	9.62 ± 0.36	12.4 ± 0.6	28.5 ± 0.7	27.8 ± 2.2	12.5 ± 1.0	28.1 ± 4.3
21	>50	>50	>50	>50	>50	>50	>50
22	>50	>50	>50	>50	>50	>50	31.5 ± 4.1
23	>50	>50	>50	>50	>50	>50	35.9 ± 13.2
24	27.2 ± 2.5	12.5 ± 1.0	34.2 ± 0.6	36.4 ± 1.9	16.3 ± 3.3	35.8 ± 3.3	24.4 ± 2.6
25	32.4 ± 4.0	30.6 ± 4.4	>50	>50	>50	39.4 ± 1.8	24.9 ± 4.5
26	8.25 ± 0.78	7.43 ± 0.57	10.3 ± 0.4	>50	17.9 ± 1.5	37.4 ± 1.7	21.4 ± 11.1
27	9.97 ± 1.01	27.1 ± 2.5	>50	>50	43.2 ± 7.2	>50	30.0 ± 4.1
Cisplatin	10.9 ± 1.6	4.42 ± 0.37	12.3 ± 0.7	11.0 ± 0.4	12.9 ± 1.9	4.8 ± 0.4	–

"–" not detected.
* Data is expressed as the mean ± SD of at least three parallel test results.

2.4. Compound **26** induces apoptosis by activating multiple caspase cascades

The apoptosis of the Bel-7402 cells caused by compound **26** was subsequently detected by flow cytometry. After treatment for 24 h with **26**, the Bel-7402 cells induced a significant dose-dependent apoptosis (Fig. 3a, b), compared with the control group. The ratios of viable cells under the treatment with doses from 10 to 40 μM were significantly diminished, while the apoptosis ratio was significantly increased in a dose-dependent manner.

In order to further understand the potential mechanism of apoptosis triggered by compound **26**, we performed western blot analysis to examine the expression of several apoptosis-related proteins. As shown in Fig. 3b and c, compound **26** treatments resulted in a decrease in the expression of Bcl-2, an increase in the expression level of Bax and cleaved-caspase-3/9 which indicated that compound **26** played a dose-dependent role in the process of caspase-3/9 activation and Bax/Bcl-2 ratio increase. Thus, these data demonstrated that compound **26** could play an initial role in apoptosis by activating multiple caspase cascades.

Many cell stress-induced apoptosis involving p38 affects the Bcl-2 protein family which includes Bax proteins that promote apoptosis and Bcl-2 proteins that resist apoptosis [28,29]. Bax protein causes altering in the permeability of mitochondrial membranes which causes the release of cytochrome *c* into the cytoplasm [30], where it forms a cytochrome *c*/Apaf-1/caspase-9 apoptotic complex and activates caspase-3 [31]. At the same time, the accumulation of ROS destroys redox homeostasis and alters the permeability of the mitochondrial membrane, ultimately stimulating the release of cytochrome *c* and inducing apoptosis [32], and Zhang [2] reported that Trx1 was demonstrated to directly inhibit cell apoptosis by catalyzing the S-nitrosylation of pro-caspase 3 and caspase 3.

2.5. Compound **26** activates the ASK1-p38-MAPK pathway

The western blot was operated for detecting the ROS-related protein status after treated with compound **26** (Fig. 4a). It has been reported that Trx1 is identified as a negative regulator of the ASK1-JNK/p38 pathway [4,33]. The reduced Trx1 could bind to ASK-1 and inactive ASK1, thereby blocking the pro-apoptotic activity of ASK-1. The oxidized Trx1 will dissociate from ASK1, thereby converting the inactive form of ASK1 into active kinase [34]. There are two main key proteins, P38 and JNK [31], in downstream of the ASK1-mediated MAPK signaling pathway. The results showed that the ratio of phosphorylated ASK1 and p38 were up-regulated significantly comparing to the control group, respectively. However, the ratio of phosphorylated JNK did not show significant differences between administration and control groups (Fig. 4b).

Altogether, compound **26** inhibited TrxR1 enzyme activity, increased the level of intracellular ROS and reduced the ratio of reduced Trx1, releasing ASK1 and activating the ASK1 pathway. Thus, **26** could activate cell apoptosis through the ROS-Trx-ASK1-p38 pathway. At the same time, apoptosis sometimes triggers p38 activation through secondary pathways, such as the production of ROS which is also a recognized activator of p38 MAPK signaling pathway [35,36].

3. Conclusions

In this study, a series of novel phenazine derivatives (**1**~**27**) containing the Michael acceptor scaffolds were designed and synthesized, in which some compounds exhibited selective cytotoxicity against Bel-7402 cancer cell lines *in vitro*. In particular, compound **26** showed better selectivity for liver cancer cells (IC_{50} = 10.3 μM for Bel-7402) comparing to MCF-7 (IC_{50} = 17.9 μM) and SGC-7901 (IC_{50} = 37.4 μM) cancer cell lines. Meanwhile, compound **26** showed no obvious cell toxicity against human normal liver epithelial L02 cells (IC_{50} > 50 μM), which means this compound possessed a better safety potential. In the following research, compound **26**, the best antiproliferative activity in this series, was verified to inhibit TrxR1 enzyme activity, ultimately resulting in cellular molecular mechanism events of apoptosis including growth of intracellular ROS, loss of reduced Trx1, liberation of ASK1 and up-regulation of p38, respectively. Together, all these evidences suggested that compound **26** acted as the TrxR1 inhibitor against Bel-7402 cancer cell line, and could activate the cells apoptosis through the ROS-Trx-ASK1-p38 pathway. The further optimization of the structure and activity of this series of compounds is being studied in our laboratory.

4. Experimental section

4.1. General

All commercially available chemicals and solvents were of analytical

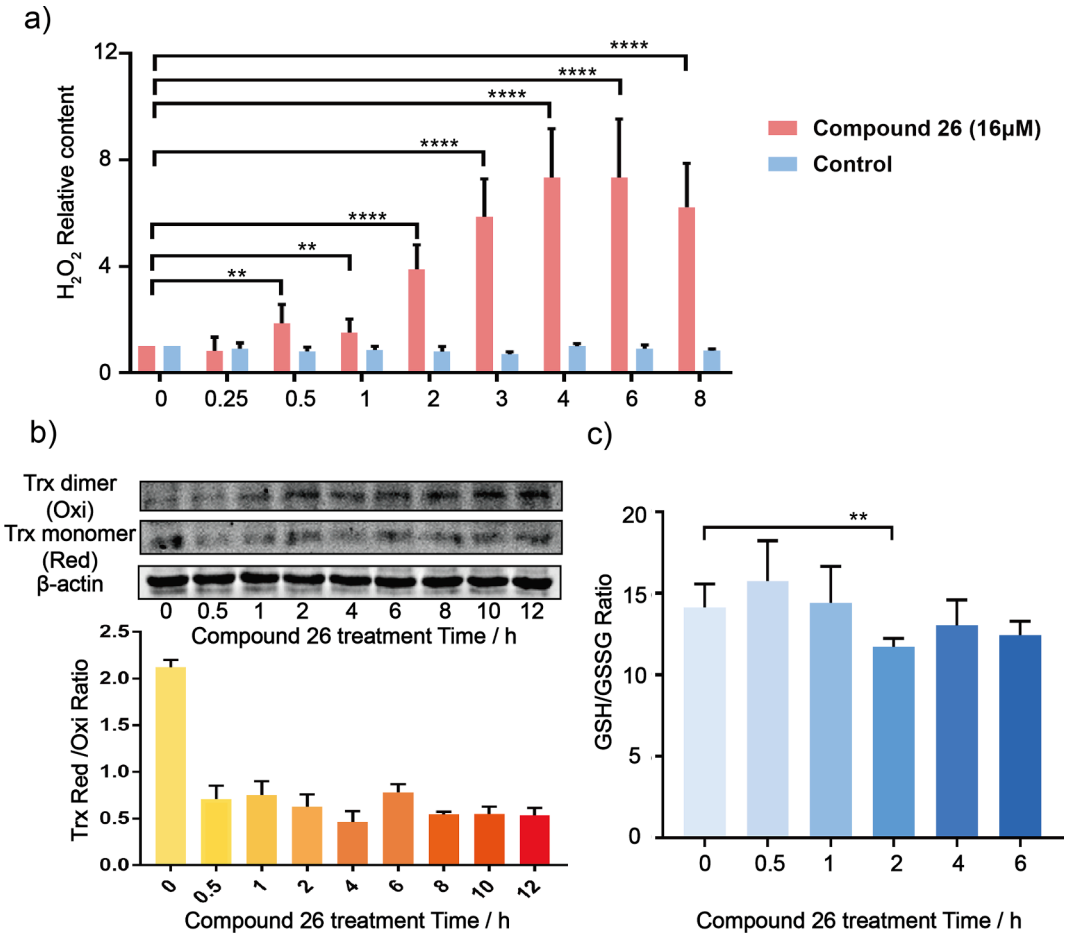

Fig. 2. Compound **26** induced the level of ROS through TrxR1-Trx1 system in Bel-7402 cancer cells. (a) 16 μM compound **26** or the same concentration of DMSO (as a solvent control) were performed to treat the cells, record the ROS (H_2O_2) levels of the cells at different times. (b) After treating the cells with 16 μM compound 26 for the corresponding time, perform non-reducing immunoblotting with the whole cell lysate, used Trx1 antibody as a probe and β-actin as control, loading 15 μg proteins in each lane, and perform quantitative processing on the results and calculate the ratio of reduced Trx1 to oxidized Trx1. (c) Treated the cells with 16 μM Compound **26**, and recorded the GSH/GSSG ratio of the cells at different times (* $p < 0.05$, ** $p < 0.01$, *** $p < 0.001$, **** $p < 0.0001$. Compared with the control group).

reagent grade and were used without further purification unless otherwise specified. Column chromatography was carried out on silica gel (100–300 mesh). TLC was conducted on silica gel 250 μm, GF254 plates with short-wavelength UV light for visualization. ^{1}H NMR and ^{13}C NMR spectroscopic measurements were performed on the Bruker AV-300 or AV-500 NMR spectrometer, using TMS as internal references at 298 K, respectively. High-resolution mass spectra (HRMS) were recorded on an Agilent 6520B UPLC-Q-TOF mass spectrometer (Agilent Technologies, Santa Clara, CA, USA). All of the products were identified by ^{1}H NMR, ^{13}C NMR and HRMS spectrometry.

4.2. General procedure for the synthesis of diverse phenazine precursors

1-methoxyphenazine, 2-amino-3-hydroxyphenazine, 2,3-dihydroxyphenazine, 1-aminophenazine, 2-aminophenazine and 2,3-diaminophenazine were prepared according to the methods described in the literature [21], [22], [23], [24], [7] and [22], respectively. After treated with BBr_3, 1-methoxyphenazine was transformed to 1-hydroxyphenazine.

4.3. General procedure for the synthesis of compounds *1~4*

Compounds **1~4** were prepared according to the procedure described as below. 1-hydroxyphenazine (196 mg, 1 mmol) was dissolved in the solution of dry CH_2Cl_2 (20 mL) and anhydrous pyridine (1 mL). Diverse acryloyl chlorides (1.5–8 mmol) diluted in CH_2Cl_2 (30 mL) then added dropwise to the above solution. The mixture was stirred under room temperature for 1–5 h, as monitored by TLC until reaction completed, and then 100 mL of CH_2Cl_2 was added, followed by washing with dilute 2 N hydrochloric acid, saturated sodium bicarbonate and water, respectively. Separating the organic layer, the solvent was removed by distillation. The residue was purified by flash chromatography on silica gel using petroleum ether/ethyl acetate (20/1–3/1, v/v), and then recrystallized with anhydrous ethanol to give the compounds **1~4**, respectively.

4.3.1. Phenazin-1-yl acrylate *1*

Yield: 41%; Yellow solid; ^{1}H NMR (500 MHz, $CDCl_3$) δ 8.33 (d, J = 8.4 Hz, 1H), 8.28–8.23 (m, 2H), 7.90–7.83 (m, 5H),7.80 (t, J = 7.8 Hz, 1H), 7.27 (d, J = 7.2 Hz, 1H); ^{13}C NMR (125 MHz, $CDCl_3$) δ 151.7, 144.2, 143.8, 141.2, 134.7, 133.2, 131.8, 130.8, 130.5, 129.7, 129.2, 127.9, 127.6, 119.9, 108.9. HR ESI-MS $[M+H]^+$ m/z = 251.0817 (calcd for $C_{15}H_{11}N_2O_2$, 251.0821).

4.3.2. Phenazin-1-yl cinnamate *2*

Yield: 47%; Reddish brown solid; ^{1}H NMR (300 MHz, $CDCl_3$) δ 8.27–8.19 (m, 3H), 8.04 (d, J = 16.0 Hz, 1H), 7.89–7.79 (m, 3H), 7.70–7.65 (m, 3H), 7.48–7.46 (m, 3H), 6.95 (d, J = 16.0 Hz, 1H); ^{13}C NMR (75 MHz, $CDCl_3$) δ 165.5, 147.2, 144.0, 143.6, 142.8, 137.5, 135.6, 134.3, 131.0, 130.8, 130.6, 130.3, 129.5, 129.5, 129.0, 129.0, 128.4,

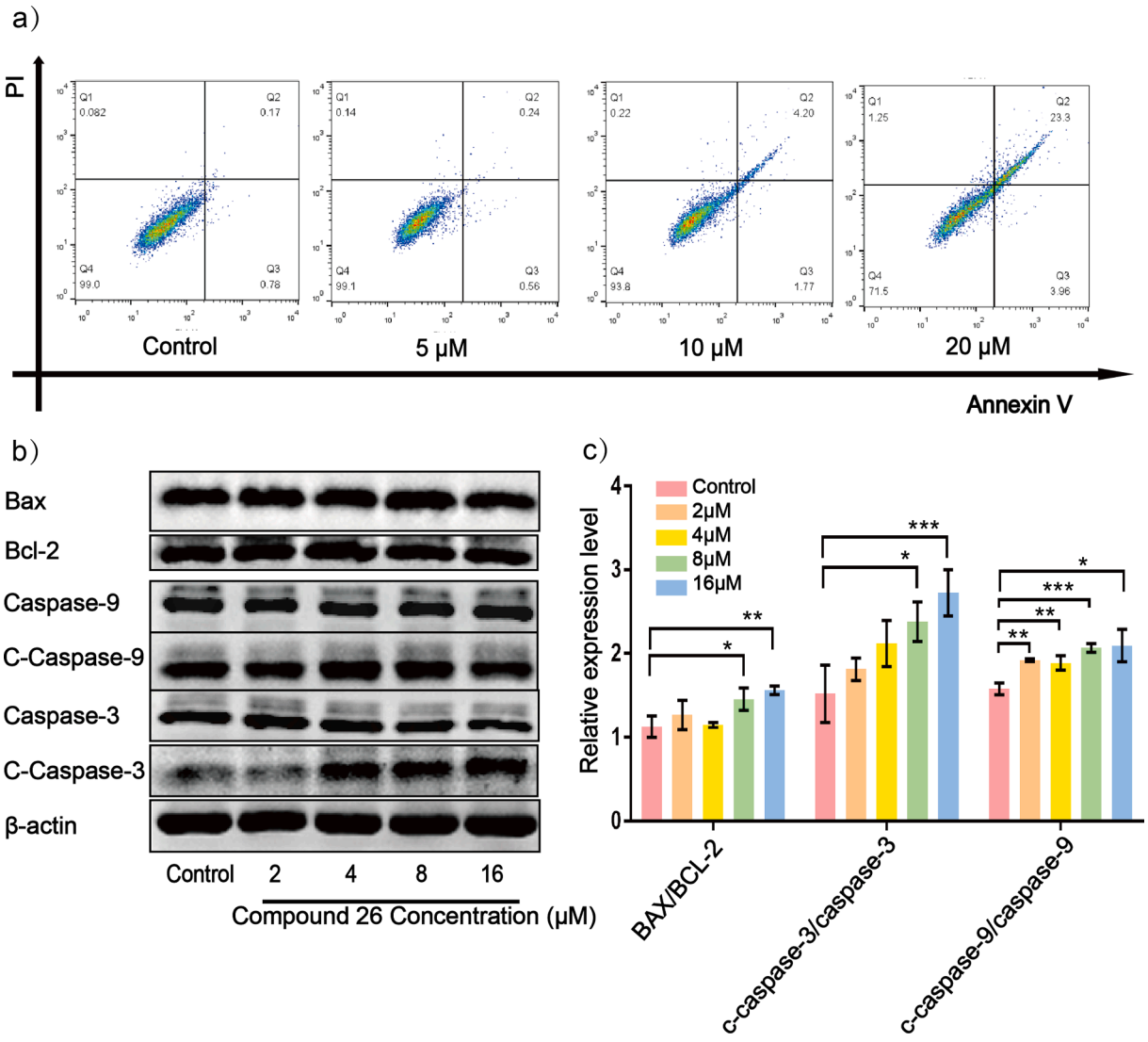

Fig. 3. Compound **26** induced caspases-depended apoptosis in Bel-7402 cancer cells. (a) The flow cytometry was applied to detect apoptosis induced by compound **26**, and calculate the percentage of apoptotic cells. (b) (c) Perform immunoblotting on the whole cell lysate and probe with Bcl-2, Bax, caspase-3/9, cleaved-caspase-3/9 antibodies, and β-actin as loading control, 15 μg proteins were loaded in each lane to quantify the results. (* $p < 0.05$, ** $p < 0.01$, *** $p < 0.001$, **** $p < 0.0001$ vs control group).

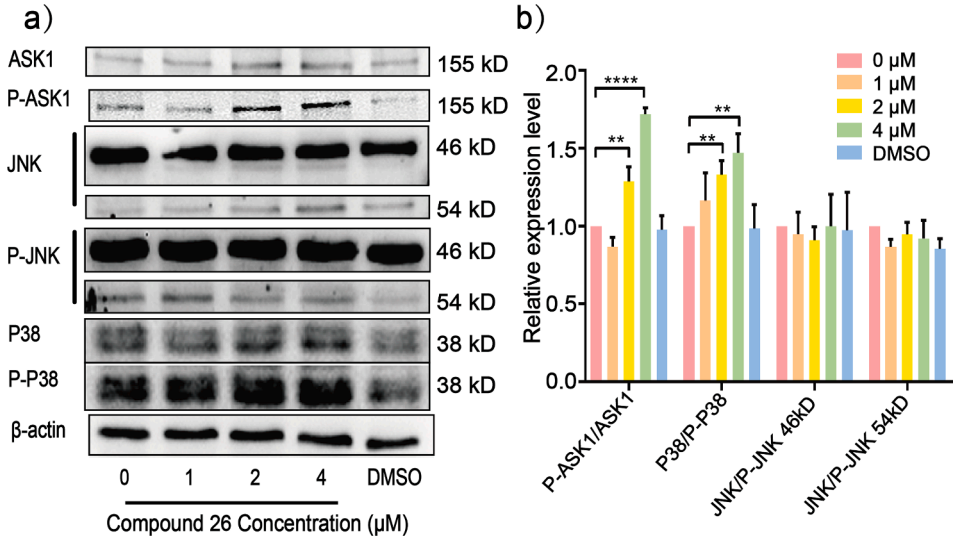

Fig. 4. Compound **26** induced cell apoptosis through ASK-1/P38 pathway in Bel-7402 cancer cells. (a) Compound **26** was incubated with Bel-7402 cells for 48 h in accordance with the concentration gradient, and whole cell lysates were applied for immunoblotting, β-actin as a loading control, and load 10 μg proteins in each lane to calculate the ratio and quantify the results (b). The means and SD of three independent experiments were performed in triplicate are shown. (* $p < 0.05$, ** $p < 0.01$, *** $p < 0.001$, **** $p < 0.0001$ vs the control group).

128.4, 127.8, 121.5, 116.9. HR ESI-MS $[M+H]^+$ m/z = 327.1141 (calcd for $C_{21}H_{15}N_2O_2$, 327.1134).

4.3.3. Phenazin-1-yl (E)-3-(3-(trifluoromethyl)phenyl)acrylate **3**

Yield: 57%; Yellow solid; ^{1}H NMR (500 MHz, $CDCl_3$) δ 8.34 (d, J = 8.5 Hz, 1H), 8.29 (t, J = 8.6 Hz, 2H), 8.07 (d, J = 16.0 Hz, 1H), 7.95 (s, 1H), 7.92–7.85 (m, 4H), 7.74 (d, J = 7.8 Hz, 1H), 7.70 (d, J = 7.2 Hz, 1H), 7.62 (t, J = 7.8 Hz, 1H), 7.03 (d, J = 16.0 Hz, 1H); ^{13}C NMR (125 MHz, $CDCl_3$) δ 164.9, 147.0, 145.4, 143.2, 142.9, 137.4, 135.0, 131.8, 131.5, 131.4, 130.9, 130.2, 130.0, 129.6, 129.0, 127.4, 127.2, 127.1, 125.0, 125.0, 121.7, 119.0. HR ESI-MS $[M+H]^+$ m/z = 395.1020 (calcd for $C_{22}H_{14}F_3N_2O_2$, 395.1007).

4.3.4. Phenazin-1-yl (E)-3-(4-fluorophenyl)acrylate **4**

Yield: 49%; Reddish brown solid; ^{1}H NMR (300 MHz, $CDCl_3$) δ 8.30 (d, J = 4.2 Hz, 1H), 8.25 (d, J = 4.2 Hz, 2H), 7.99 (d, J = 8.0 Hz, 1H), 7.90–7.82 (m, 3H), 7.68–7.66 (m, 3H), 7.15 (t, J = 4.2 Hz, 2H), 6.86 (d, J = 8.0 Hz, 1H); ^{13}C NMR (75 MHz, $CDCl_3$) δ 165.9, 165.4, 147.1, 145.9, 143.9, 143.5, 143.1, 137.4, 131.1, 130.7, 130.4, 130.3, 130.2, 129.6, 129.4, 127.8, 121.5, 116.7, 116.7, 116.4, 116.1. HR ESI-MS $[M+H]^+$ m/z = 345.1047 (calcd for $C_{21}H_{14}FN_2O_2$, 345.1039).

4.4. General procedure for the synthesis of compounds **5~8**

Compounds **5~8** were prepared with the similar method of preparing compounds **1~4**. 2-amino-3-hydroxyphenazine was used in place of 1-hydroxyphenazine as the reactant to get compounds **5~8**.

4.4.1. 3-aminophenazin-2-yl acrylate **5**

Yield: 61%; Reddish brown solid; ^{1}H NMR (300 MHz, DMSO-d_6) δ 7.92 (s, 2H), 7.59 (s, 2H), 7.01–6.95 (m, 2H), 6.31 (s, 2H), 6.52 (dd, J = 17.0, 10.0 Hz, 1H), 6.38 (dd, J = 17.0, 2.0 Hz, 1H), 5.86 (dd, J = 10.0, 2.0 Hz, 1H); ^{13}C NMR (75 MHz, DMSO-d_6) δ 164.3, 146.5, 144.2, 142.2, 141.3, 140.4, 134.6, 132.1, 130.8, 130.0, 128.2, 127.1, 126.3, 125.3, 110.5. HR ESI-MS $[M+H]^+$ m/z = 266.0937 (calcd for $C_{15}H_{12}N_3O_2$, 266.0930).

4.4.2. 3-aminophenazin-2-yl (E)-but-2-enoate **6**

Yield: 65%; Reddish brown solid; ^{1}H NMR (300 MHz, DMSO-d_6) δ 7.94 (s, 2H), 7.57 (s, 2H), 7.03–6.98 (m, 2H), 6.33 (s, 2H), 6.07–6.03 (m, 1H), 5.85 (dd, J = 15.2, 1.7 Hz, 1H), 1.95 (dd, J = 6.9, 1.4 Hz, 3H); ^{13}C NMR (75 MHz, DMSO-d_6) δ 164.6, 146.4, 144.6, 142.5, 141.2, 140.6, 134.3, 132.5, 130.6, 130.1, 128.5, 127.2, 126.5, 125.1, 114.6, 18.3. HR ESI-MS $[M+H]^+$ m/z = 280.1074 (calcd for $C_{16}H_{14}N_3O_2$, 280.1086).

4.4.3. 3-aminophenazin-2-yl 3-methylbut-2-enoate **7**

Yield: 62%; Reddish brown solid; ^{1}H NMR (300 MHz, DMSO-d_6) δ 7.92 (s, 2H), 7.56 (s, 2H), 7.00–6.96 (m, 2H), 6.30 (s, 2H), 6.55 (s, 1H), 2.16 (s, 3H), 1.93 (s, 3H); ^{13}C NMR (75 MHz, DMSO-d_6) δ 164.6, 146.4, 144.6, 142.5, 141.2, 140.6, 134.3, 132.5, 130.6, 130.1, 128.5, 127.2, 126.5, 125.1, 114.6, 26.5, 19.1. HR ESI-MS $[M+H]^+$ m/z = 294.1252 (calcd for $C_{17}H_{16}N_3O_2$, 294.1243).

4.4.4. 3-aminophenazin-2-yl methacrylate **8**

Yield: 71%; Reddish brown solid; ^{1}H NMR (300 MHz, DMSO-d_6) δ 7.89 (s, 2H), 7.60 (s, 2H), 7.01–6.97 (m, 2H), 6.35 (s, 2H), 6.44 (d, J = 11.2 Hz, 1H), 6.21 (d, J = 10.2 Hz, 1H), 2.03 (s, 3H); ^{13}C NMR (75 MHz, DMSO-d_6) δ 165.3, 146.8, 144.3, 143.2, 141.9, 140.8, 135.3, 133.4, 131.2, 130.4, 128.8, 127.5, 126.2, 125.7, 112.6, 18.3. HR ESI-MS $[M+H]^+$ m/z = 280.1093 (calcd for $C_{16}H_{14}N_3O_2$, 280.1086).

4.5. General procedure for the synthesis of compounds **9~11**

Compounds **9~11** were prepared with the similar method of preparing compounds **1~4**. 2,3-dihydroxyphenazine was used in place of 1-hydroxyphenazine as the reactant to get compounds **9~11**.

4.5.1. Phenazine-2,3-diyl diacrylate **9**

Yield: 61%; Reddish brown solid; ^{1}H NMR (300 MHz, DMSO-d_6) δ 8.72 (s, 2H), 8.25 (dd, J = 6.6, 3.4 Hz, 2H), 7.92 (dd, J = 6.6, 3.4 Hz, 2H), 6.58 (dd, J = 17.0, 10.0 Hz, 2H), 6.44 (dd, J = 17.0, 2.1 Hz, 2H), 5.83 (dd, J = 10.0, 2.1 Hz, 2H); ^{13}C NMR (75 MHz, DMSO-d_6) δ 165.4, 165.4, 144.7, 144.7, 142.8, 142.8, 141.9, 141.9, 136.1, 136.1, 131.2, 131.2, 129.7, 129.7, 126.8, 126.8, 120.6, 120.6. HR ESI-MS $[M+H]^+$ m/z = 321.0881 (calcd for $C_{18}H_{13}N_2O_4$, 321.0875).

4.5.2. Phenazine-2,3-diyl (2E,2′E)-bis(but-2-enoate) **10**

Yield: 65%; Reddish brown solid; ^{1}H NMR (300 MHz, DMSO-d_6) δ 8.74 (s, 2H), 8.22 (dd, J = 6.7, 3.4 Hz, 2H), 7.89 (dd, J = 6.7, 3.4 Hz, 2H), 7.03–6.94 (m, 2H), 6.43 (dd, J = 15.3, 1.8 Hz, 2H), 1.97 (dd, J = 6.9, 1.8 Hz, 6H); ^{13}C NMR (75 MHz, DMSO-d_6) δ 165.6, 165.6, 144.5, 144.5, 142.6, 142.6, 141.7, 141.7, 136.5, 136.5, 131.7, 131.7, 129.4, 129.4, 126.5, 126.5, 120.4, 120.4, 18.3, 18.3. HR ESI-MS $[M+H]^+$ m/z = 349.1182 (calcd for $C_{20}H_{17}N_2O_4$, 349.1188).

4.5.3. Phenazine-2,3-diyl bis(3-methylbut-2-enoate) **11**

Yield: 59%; Reddish brown solid; ^{1}H NMR (300 MHz, DMSO-d_6) δ 8.75 (s, 2H), 8.19 (dd, J = 6.7, 3.3 Hz, 2H), 7.90 (dd, J = 6.7, 3.3 Hz, 2H), 6.58 (s, 2H), 2.21 (s, 6H), 1.97 (s, 6H); ^{13}C NMR (75 MHz, DMSO-d_6) δ 164.7, 164.7, 145.1, 145.1, 142.5, 142.5, 141.4, 141.4, 136.8, 136.8, 132.2, 132.2, 129.7, 129.7, 126.3, 126.3, 116.8, 116.8, 26.8, 26.8, 19.3, 19.3. HR ESI-MS $[M+H]^+$ m/z = 377.1509 (calcd for $C_{22}H_{21}N_2O_4$, 377.1501).

4.6. General procedure for the synthesis of compounds **12~15**

Compounds **12~15** were prepared with the similar method of preparing compounds **1~4**. 1-aminophenazine was used in place of 1-hydroxyphenazine as the reactant to get compounds **12~15**.

4.6.1. N-(phenazin-1-yl)acrylamide **12**

Yield: 73%; Yellow solid; ^{1}H NMR (500 MHz, $CDCl_3$) δ 9.95 (s, 1H), 8.93 (d, J = 7.5 Hz, 1H), 8.29–8.25 (m, 2H), 7.96 (d, J = 8.7 Hz, 1H), 7.89–7.85 (m, 3H), 6.60 (d, J = 5.6 Hz, 2H), 5.93 (t, J = 5.7 Hz, 1H); ^{13}C NMR (125 MHz, $CDCl_3$) δ 163.8, 143.8, 143.1, 142.2, 134.7, 134.0, 131.7, 131.5, 130.8, 130.7, 129.6, 129.2, 128.1, 123.4, 116.4. HR ESI-MS $[M+H]^+$ m/z = 250.0992 (calcd for $C_{15}H_{12}N_3O$, 250.0980).

4.6.2. N-(phenazin-1-yl)cinnamamide **13**

Yield: 54%; Yellow solid; ^{1}H NMR (500 MHz, $CDCl_3$) δ 10.00 (s, 1H), 8.99 (d, J = 7.5 Hz, 1H), 8.32 (dt, J = 6.6, 3.4 Hz, 2H), 7.98 (d, J = 8.8 Hz, 1H), 7.92–7.88(m, 4H), 7.69 (d, J = 6.9 Hz, 2H), 7.48–7.43 (m, 3H), 6.90 (d, J = 15.6 Hz, 1H); ^{13}C NMR (125 MHz, $CDCl_3$) δ 164.2, 143.7, 143.1, 142,8, 142.8, 141.2, 134.7, 134.3, 131.9, 130.8, 130.7, 130.1, 129.6, 129.2, 128.9, 128.9, 128.1, 128.1, 123.2, 121.1, 116.4. HR ESI-MS $[M+H]^+$ m/z = 326.1287 (calcd for $C_{21}H_{16}N_3O$, 326.1293).

4.6.3. (E)-N-(phenazin-1-yl)-3-(3-(trifluoromethyl)phenyl)acrylamide **14**

Yield: 65%; Yellow solid; ^{1}H NMR (500 MHz, $CDCl_3$) δ 10.04 (s, 1H), 8.99 (d, J = 7.4 Hz, 1H), 8.35–8.31 (m, 2H), 7.99 (d, J = 8.8 Hz, 1H), 7.94 (d, J = 5.2 Hz, 1H), 7.93–7.87 (m, 4H), 7.83 (d, J = 7.6 Hz, 1H), 7.69 (d, J = 7.6 Hz, 1H), 7.59 (t, J = 7.8 Hz, 1H), 6.97 (d, J = 15.5 Hz, 1H); ^{13}C NMR (125 MHz, $CDCl_3$) δ 163.6, 143.8, 143.1, 141.2, 141.1, 135.2, 134.7, 134.1, 131.8, 131.5, 130.9, 130.8, 129.6, 129.5, 129.2, 126.5, 126.5, 124.3, 124.3, 123.5, 123.0, 116.5. HR ESI-MS $[M+H]^+$ m/z = 394.1178 (calcd for $C_{22}H_{15}F_3N_3O$, 394.1167).

4.6.4. (E)-3-(4-fluorophenyl)-N-(phenazin-1-yl)acrylamide **15**

Yield: 69%; Yellow solid; ^{1}H NMR (500 MHz, $CDCl_3$) δ 9.98 (s, 1H), 8.98 (d, J = 7.3 Hz, 1H), 8.33–8.29 (m, 2H), 7.97 (d, J = 8.5 Hz, 1H), 7.92–7.84 (m, 4H), 7.67 (dd, J = 8.4, 5.5 Hz, 2H), 7.15 (t, J = 8.5 Hz, 2H), 6.82 (d, J = 15.5 Hz, 1H); ^{13}C NMR (125 MHz, $CDCl_3$) δ 164.8, 164.1, 162.8, 143.8, 143.1, 141.6, 141.2, 134.7, 134.2, 131.8, 130.8,

130.7, 130.0, 130.0, 129.6, 129.2, 123.26, 120.8, 116.4, 116.2, 116.0. HR ESI-MS $[M+H]^+$ m/z = 344.1187 (calcd for $C_{21}H_{15}FN_3O$, 344.1199).

4.7. General procedure for the synthesis of compounds **16~20**

Compounds **16~20** were prepared with the similar method of preparing compounds **1~4**. 2-aminophenazine was used in place of 1-hydroxyphenazine as the reactant to get compounds **16~20**.

4.7.1. N-(phenazin-2-yl)acrylamide **16**

Yield: 41%; Reddish brown solid; ^{1}H NMR (300 MHz, DMSO-d_6) δ 10.79 (s, 1H), 8.81 (d, J = 2.2 Hz, 1H), 8.23 (m, 3H), 8.02 (dd, J = 9.4, 2.3 Hz, 1H),7.97–7.87 (m, 2H), 6.57 (dd, J = 17.0, 10.0 Hz, 1H), 6.40 (dd, J = 17.0, 2.0 Hz, 1H), 5.90 (dd, J = 10.0, 2.0 Hz, 1H); ^{13}C NMR (75 MHz, DMSO-d_6) δ 164.5, 144.3, 143.7, 142.4, 141.0, 141.0, 131.9, 131.4, 130.4, 130.4, 129.8, 129.4, 128.6, 126.8, 114.7. HR ESI-MS $[M+H]^+$ m/z = 250.0972 (calcd for $C_{15}H_{12}N_3O_1$, 250.0980).

4.7.2. (E)-N-(phenazin-2-yl)but-2-enamide **17**

Yield: 38%; Reddish brown solid; ^{1}H NMR (300 MHz, DMSO-d_6) δ 10.59 (s, 1H), 8.77 (d, J = 2.2 Hz, 1H), 8.23–8.18 (m, 3H), 8.00 (dd, J = 9.4, 2.3 Hz, 1H), 7.95–7.86 (m, 2H), 6.99–6.89 (m, 1H), 6.25 (dd, J = 15.2, 1.7 Hz, 1H), 1.93 (dd, J = 6.9, 1.4 Hz, 3H); ^{13}C NMR (75 MHz, DMSO-d_6) δ 164.8, 144.3, 143.6, 142.3, 141.9, 141.9, 141.3, 140.9, 131.3, 130.3, 129.7, 129.4, 126.9, 126.0, 114.3, 18.1. HR ESI-MS $[M+H]^+$ m/z = 264.1144 (calcd for $C_{16}H_{14}N_3O$, 264.1137).

4.7.3. N-(phenazin-2-yl)cinnamamide **18**

Yield: 43%; Reddish brown solid; ^{1}H NMR (300 MHz, DMSO-d_6) δ 10.86 (s, 1H), 8.85 (s, 1H), 8.26–8.20 (m, 3H), 8.05–7.99 (m, 1H), 7.91–7.85 (m, 2H), 7.72–7.65 (m, 3H), 7.27–7.20 (m, 2H), 7.23 (d, J = 7.2 Hz, 1H), 6.96 (d, J = 15.6 Hz, 1H); ^{13}C NMR (75 MHz, DMSO-d_6) δ 165.6, 155.4, 144.7, 144.1, 141.7, 141.2, 139.8, 135.8, 134.4, 131.5, 130.6, 129.3, 129.0, 128.5, 126.7, 122.5, 120.2, 116.4, 115.4, 114.1, 107.6. HR ESI-MS $[M+H]^+$ m/z = 326.1283 (calcd for $C_{21}H_{16}N_3O$, 326.1293).

4.7.4. (E)-N-(phenazin-2-yl)-3-(3-(trifluoromethyl)phenyl)acrylamide **19**

Yield: 44%; Reddish brown solid; ^{1}H NMR (300 MHz, DMSO-d_6) δ 10.9 (s, 1H), 8.87 (d, J = 2.1 Hz, 1H), 8.27–8.21 (m, 3H), 8.06–8.05 (m, 2H), 8.02–7.97 (m, 2H), 7.96–7.90 (m, 2H), 7.82–7.80 (m, 1H), 7.73 (t, J = 7.7 Hz, 1H), 7.08 (d, J = 15.8 Hz, 1H); ^{13}C NMR (75 MHz, DMSO-d_6) δ 164.6, 144.4, 143.7, 142.4, 141.2, 141.1, 140.0, 136.2, 132.2, 131.5, 130.7, 130.6, 130.5, 130.2, 130.1, 129.8, 129.4, 126.8, 124.7, 124.7, 124.4, 114.6. HR ESI-MS $[M+H]^+$ m/z = 394.1175 (calcd for $C_{22}H_{15}F_3N_3O$, 394.1167).

4.7.5. (E)-3-(4-fluorophenyl)-N-(phenazin-2-yl)acrylamide **20**

Yield: 37%; Reddish brown solid; ^{1}H NMR (300 MHz, DMSO-d_6) δ 10.83 (s, 1H), 8.83 (s, 1H), 8.23–8.19 (m, 3H), 8.03 (dd, J = 9.4, 1.7 Hz, 1H), 7.90 (m, 2H), 7.77–7.70 (m, 3H), 7.30 (t, J = 8.7 Hz, 2H), 6.88 (d, J = 15.7 Hz, 1H); ^{13}C NMR (75 MHz, DMSO-d_6) δ 164.9, 144.4, 143.7, 142.4, 141.3, 141.0, 140.7, 131.7, 131.7, 131.4, 130.7, 130.6, 130.5, 130.4, 129.8, 129.4, 126.9, 122.0, 116.6, 116.5, 114.4. HR ESI-MS $[M+H]^+$ m/z = 344.1208 (calcd for $C_{21}H_{15}FN_3O$, 344.1199).

4.8. General procedure for the synthesis of compounds **21~23**

Compounds **21~23** were prepared with the similar method of preparing compounds **1~4**. 2,3-diaminophenazine was used in place of 1-hydroxyphenazine as the reactant to get compounds **21~23**.

4.8.1. N,N'-(phenazine-2,3-diyl)diacrylamide **21**

Yield: 47%; Red powder; ^{1}H NMR (300 MHz, DMSO-d_6) δ 9.85 (s, 2H), 8.71 (s, 2H), 8.24 (dd, J = 6.7, 3.3 Hz, 2H), 7.90 (dd, J = 6.7, 3.3 Hz, 2H), 6.59 (dd, J = 17.0, 10.0 Hz, 2H), 6.43 (dd, J = 17.0, 2.2 Hz, 2H), 5.92 (dd, J = 10.0, 2.2 Hz, 2H); ^{13}C NMR (75 MHz, DMSO-d_6) δ 165.8, 165.8, 144.7, 144.7, 142.5, 142.5, 141.7, 141.7, 136.1, 136.1, 131.4, 131.4, 129.5, 129.5, 126.8, 126.8, 120.4, 120.4. HR ESI-MS $[M+H]^+$ m/z = 319.1190 (calcd for $C_{18}H_{15}N_4O_2$, 319.1195).

4.8.2. (2E,2'E)-N,N'-(phenazine-2,3-diyl)bis(but-2-enamide) **22**

Yield: 30%; Red powder; ^{1}H NMR (300 MHz, DMSO-d_6) δ 9.88 (s, 2H), 8.67 (s, 2H), 8.20 (dd, J = 6.7, 3.4 Hz, 2H), 7.90 (dd, J = 6.7, 3.4 Hz, 2H), 7.01–6.89 (m, 2H), 6.39 (dd, J = 15.3, 1.8 Hz, 2H), 1.94 (dd, J = 6.9, 1.8 Hz, 6H); ^{13}C NMR (75 MHz, DMSO-d_6) δ 164.9, 164.9, 143.1, 143.1, 141.6, 141.6, 141.4, 141.4, 135.0, 135.0, 130.7, 130.7, 129.5, 129.5, 126.4, 126.4, 120.4, 120.4, 18.1, 18.1. HR ESI-MS $[M+H]^+$ m/z = 347.1509 (calcd for $C_{20}H_{19}N_4O_2$, 347.1508).

4.8.3. N,N'-(phenazine-2,3-diyl)bis(3-methylbut-2-enamide) **23**

Yield: 41%; Red powder; ^{1}H NMR (300 MHz, DMSO-d_6) δ 9.85 (s, 2H), 8.73 (s, 2H), 8.22 (dd, J = 6.8, 3.4 Hz, 2H), 7.92 (dd, J = 6.8, 3.4 Hz, 2H), 6.56 (s, 2H), 2.24 (s, 6H), 1.98 (s, 6H); ^{13}C NMR (75 MHz, DMSO-d_6) δ 165.2, 165.2, 145.4, 145.4, 143.3, 143.3, 141.7, 141.7, 136.5, 136.5, 132.6, 132.6, 129.7, 129.7, 126.5, 126.5, 116.6, 116.6, 26.7, 26.7, 19.5, 19.5. HR ESI-MS $[M+H]^+$ m/z = 375.1828 (calcd for $C_{22}H_{23}N_4O_2$, 375.1821).

4.9. General procedure for the synthesis of compounds **24~27**

1,4-phenylenediamine was used as the starting material to synthesize 6-methoxy-2-aminophenazine following the modified method in the literature [21], which subsequently reacted with diverse acryloyl chlorides to prepare compounds **24~27** with the similar method of preparing compounds **1~4**.

4.9.1. N-(6-methoxyphenazin-2-yl)acrylamide **24**

Yield: 41%; Orange solid; ^{1}H NMR (500 MHz, DMSO-d_6) δ 10.76 (s, 1H), 8.75 (s, 1H), 8.24 (d, J = 9.3 Hz, 1H), 7.99 (dd, J = 9.3, 2.2 Hz, 1H), 7.84–7.80 (m, 1H), 7.72 (d, J = 8.7 Hz, 1H), 7.21 (d, J = 7.4 Hz, 1H), 6.56 (dd, J = 16.9, 10.1 Hz, 1H), 6.40 (d, J = 17.0 Hz, 1H), 5.93–5.85 (m, 1H), 4.06 (s, 3H); ^{13}C NMR (125 MHz, DMSO-d_6) δ 164.6, 155.6, 144.4, 144.1, 141.2, 139.6, 135.6, 131.9, 131.7, 130.8, 128.7, 126.3, 120.7, 114.5, 107.1, 56.4. HR ESI-MS $[M+H]^+$ m/z = 280.1079 (calcd for $C_{16}H_{14}N_3O_2$, 280.1086).

4.9.2. N-(6-methoxyphenazin-2-yl)cinnamamide **25**

Yield: 42%; Reddish brown solid; ^{1}H NMR (300 MHz, DMSO-d_6) δ 10.83 (s, 1H), 8.80 (d, J = 2.0 Hz, 1H), 8.25 (d, J = 9.4 Hz, 1H), 8.01 (dd, J = 9.4, 2.2 Hz, 1H), 7.85–7.80 (m, 1H), 7.75–7.68 (m, 4H), 7.50–7.44 (m, 3H), 7.21 (d, J = 7.2 Hz, 1H), 6.94 (d, J = 15.7 Hz, 1H), 4.06 (s, 3H); ^{13}C NMR (75 MHz, DMSO-d_6) δ 165.0, 155.6, 144.5, 144.3, 141.9, 141.5, 139.7, 135.6, 135.0, 131.7, 130.8, 130.6, 129.6, 128.4, 126.3, 122.2, 120.8, 116.1, 115.1, 114.3, 107.1, 56.5. HR ESI-MS $[M+H]^+$ m/z = 356.1395 (calcd for $C_{22}H_{18}N_3O_2$, 356.1399).

4.9.3. (E)-N-(6-methoxyphenazin-2-yl)-3-(3-(trifluoromethyl)phenyl) acrylamide **26**

Yield: 45%; Reddish brown solid; ^{1}H NMR (500 MHz, DMSO-d_6) δ 10.91 (s, 1H), 8.82 (d, J = 2.3 Hz, 1H), 8.27 (d, J = 9.3 Hz, 1H), 8.06 (s, 1H), 8.01 (dd, J = 9.2, 2.4 Hz, 2H), 7.85–7.80 (m, 3H), 7.75–7.71 (m, 2H), 7.23 (d, J = 7.7 Hz, 1H), 7.07 (d, J = 9.7 Hz, 1H), 4.07 (s, 3H); ^{13}C NMR (125 MHz, DMSO-d_6) δ 164.5, 155.6, 144.5, 144.2, 141.4, 140.0, 139.7, 136.2, 135.6, 132.2, 131.7, 130.9, 130.7, 126.8, 126.7, 126.2, 124.7, 124.6, 124.4, 120.8, 114.4, 107.1, 56.5. HR ESI-MS $[M+H]^+$ m/z = 424.1288 (calcd for $C_{23}H_{17}F_3N_3O_2$, 424.1273).

4.9.4. (E)-3-(4-fluorophenyl)-N-(6-methoxyphenazin-2-yl)acrylamide **27**

Yield: 42%; Reddish brown solid; ^{1}H NMR (300 MHz, DMSO-d_6) δ 10.84 (s, 1H), 8.81 (d, J = 2.2 Hz, 1H), 8.27 (d, J = 9.3 Hz, 1H), 8.01 (dd, J = 9.4, 2.4 Hz, 1H), 7.87–7.72 (m, 5H), 7.33 (t, J = 9.0 Hz, 2H), 7.23

(dd, $J = 7.7$, 1.2 Hz, 1H), 6.89 (d, $J = 15.8$ Hz, 1H), 4.07 (s, 3H); ^{13}C NMR (75 MHz, DMSO-d_6) δ 164.9, 155.7, 144.5, 144.3, 141.5, 140.7, 139.7, 135.6, 131.7, 130.9, 130.7, 130.6, 130.1, 126.3, 122.1, 122.0, 120.8, 116.7, 116.5, 114.3, 107.1, 56.5. HR ESI-MS $[M+H]^+$ m/z = 374.1308 (calcd for $C_{22}H_{17}FN_3O_2$, 374.1305).

4.10. Cell culture and reagents

MTT (Cat.# S19063, YuanyeBio, Shanghai, China), DMSO (Cat.# 30072418, SCR, Cina), RIPA (Cat.# P0013B) (Beyotime, China), Dual Color Prestained Protin Marker (Cat.# WJ101) (EpiZyme, China). Antibody against Bcl-2 (Cat.# AF6139), Bax (Cat.# AF0120), Caspase 9 (Cat.# AF6348), Cleaved-Caspase 3 (Asp 175) (Cat.# AF7022), Ask1 (Cat.# AF6477), Phospho-Ask1 (Thr838) (Cat.# AF8096) was from Affinity. Antibody against Caspase-3 (Cat.# LTO6560), Cleaved-Caspase 9 (D330) (Cat.# LTO3100C), JNK1/2/3 (Cat.# LTO9342), Phospho-JNK1/2/3 (T183/Y185) (Cat.# LTO7510P), P38 (Cat.# LTO3153), Phospho-P38 (Cat.# LTO8380P) was from Litho. Antibody against Thioredoxin (Cat.# 14999–1-AP) from proteinech.

Cells were cultured in medium with 10% (v/v) fetal bovine serum (FBS) (Gibco, Grand Island, NY, USA), 100 μg/ml streptomycin, and 100 units/ml penicillin. in a 5% CO_2 incubator at 37 °C. The human liver cancer cell lines, HepG2 (Cat.# KG020) cell line was obtained from ATCC, KeyGEN BioTECH, China. HuH-7 (Cat.# FH05946), Bel-7402 (Cat.# FH98464) and MCF-7 cell line purchased from FuHeng Cell Center, Shanghai, China. Human gastric cancer cell lines SGC-7901 was obtained from China academia Sinica Cell repository (Shanghai). HuH-7 and MCF-7 cells preserved were cultured in high glucose DMEM medium (KeyGEN BioTECH, China). HepG2 cells preserved were cultured in MEM medium (KeyGEN BioTECH, China). Bel-7402, SCG-7901 and L02 cells preserved were cultured in 1640 medium (KeyGEN BioTECH, China).

4.11. Cytotoxic activity in vitro

The cytotoxic activities of compounds *in vitro* were measured using the 3-(4,5-Dimethylthiazole)-2,5-diphenyltetraazolium bromide (MTT) assay. Cells in the form of cell suspension were placed in 96-well plates (4×10^3 cells per well) and grown overnight at 37 °C in a 5% CO_2 incubator. The tested compounds were dissolved in DMSO and then added to the wells to achieve final concentrations ranging from 5 to 40 μM after serial dilution. Blank controls were prepared by addition of culture medium (200 μL). The solvent control group was added with medium containing the corresponding concentration of DMSO. The plates were incubated at 37 °C in a 5% CO_2 incubator for 48 h. At the end of the treatment, 20 μL MTT solutions (5 mg/mL) were added to each well and incubated for 4 h at 37 °C, then 150 μL DMSO was added to solubilize the MTT formazan after removing the original medium, respectively. The optical density of each well was measured with a microplate reader at a wavelength of 490 nm. Each experiment was repeated at least three times to obtain the mean values. Five different tumor cell lines and one normal hepatocyte are the subjects of this study: HepG2, HuH-7, Bel-7402, MCF-7, SCG-7901 and L02.

4.12. Detection of TrxR1 enzyme activities

The TrxR1 enzyme activity kit (Cat.# BC1155, Solarbio) was applied to perform TrxR1 enzyme activity detection. The Bel-7402 cells were directly sonicated (300 w, ultrasound 3 s, interval 7 s, total time 3 min) before administration, the total protein was extracted in the cell by centrifuge (12,000 rpm, 15 min). Then, the different concentrations of the compounds and the protein supernatants were incubated in 37 °C for 30 min. After the incubation, the subsequent enzyme activity tests were carried out according to the instructions, and the enzyme activities results of the different doses calculate EC_{50}.

4.13. Flow cytometry analysis

Using flow cytometry (BD FACS Accuri C6) to determine and analyze the apoptosis of the tested cells. Collect cells treated with different concentrations of compound **26** for 24 h, and detect the apoptosis of cells treated with compound **26** according to the steps of Annexin V-PI Apoptosis Detection Kit (Cat. # Y6002, US EVERBRIGHT). FACS analysis was performed to determine the cell cycle distribution and the percentage of apoptotic cells.

4.14. Hydrogen peroxide assay

Use a Hydrogen Peroxide Assay Kit (Cat.# S0038, Beyotime) to detect the concentration of hydrogen peroxide of the cell. Bel-7402 cells were seeded into six-well plates at a density of 2×10^5 cells per well and incubated for 24 h. Subsequently, the corresponding concentration of the compounds were diluted with medium, and added to the six-well plate at the corresponding time, cultured in a 5% CO_2 incubator at 37 °C. The cells were collected and centrifuged at 3500 rpm for 5 min at 4 °C. After discarding the supernatant, 150 μL of hydrogen peroxide detection lysate per 1 million cells were added to the lysate, then homogenized thoroughly to break and lyse the cells and centrifuged at 12,000 rpm at 4 °C for 5 min to take the supernatant for subsequent determination. The supernatant of cultured cells were used directly for subsequent determinations. A 96-well plate was used for detection. Add 50 μL of the sample to be tested or standard to each well, and then add 100 μL of hydrogen peroxide detection reagent (containing Fe^{2+} and xylenol orange), mix well and place at room temperature for 30 min, and then immediately determine at 560 nm. The concentration of hydrogen peroxide was calculated in the sample according to the standard curve.

4.15. GSH and GSSH assay

Use GSH and GSSH Assay Kit (Cat.# S0053, Beyotime) to detect the content of GSH and GSSH inside the cell. BEL-7402 cells were seeded into six-well plates at a density of 2×10^5 cells per well and incubated for 24 h. Subsequently, the compound was diluted with the medium to the corresponding concentration, and added to the six-well plate at the corresponding time, and the cells were cultured at 37 °C in a 5% CO_2 incubator. At the same time, prepare test reagents according to the instructions of the kit. After the corresponding co-cultivation time, collect the cells, add the protein removal reagent M solution according to the ratio of 1:3 (v/v) and vortex. After two quick freezing and thawing with liquid nitrogen and 37 °C water baths, centrifuging to obtain the total glutathione determination samples (supernatant). To prepare GSSG test samples, add 20 μL of diluted GSH removal auxiliary solution per 100 μL samples, and then add GSH removal working solution according to the proportion of 4 μL per 100 μL samples for vortexing and settled sample at 25 °C for 60 min. Subsequently, the total glutathione and GSSG content were determined according to the instructions, and the GSH content was calculated according to the measurement results.

4.16. Western blot analysis

Bel-7402 cells were seeded into six-well plates at a density of 2×10^5 cells per well and incubated for 24 h. Subsequently, the compounds were diluted with the medium to the corresponding concentration, and incubated with the cells at 37 °C in a 5% CO_2 incubator. The cells were collected and after centrifugation at 3000 rpm at 4 °C, and the cells were lysed with RIPA added with PMSF and a phosphatase inhibitor. After being lysed on ice for 30 min, the samples were centrifuged at 4 °C and 12,000 rpm for 15 min. The supernatant contained protein. The protein concentration of the supernatant was determined by BCA assay. Determine the loading amount according to the BCA results, so that the protein loading amount of each lane of sodium dodecyl sulfate–polyacrylamide gel electrophoresis (SDS-PAGE) is equal. Then add

loading buffer to the sample, which contains (for reducing SDS-PAGE) or without (for non-reducing SDS-PAGE) reducing agents such as DDT. Gels were then transferred to PVDF membranes and blocked with Protein Free Rapid Blocking Buffer for 30 min. Then the membranes were incubated with primary antibodies at 1:1000 dilutions in 5% BSA overnight at 4 °C. After 12 h, the strips were washed three times with TBST for a total of 30 min. After that, the secondary antibody was conjugated in a 1:5000 dilution at room temperature for 45 min, and then washed with TBST 3 times, each for 10 min. Levels of a β-actin, used as loading control were also quantified to confirm equal protein loading on the gels.

Declaration of Competing Interest

The authors declare that they have no known competing financial interests or personal relationships that could have appeared to influence the work reported in this paper.

Acknowledgements

The study received financial support from the National Science and Technology Major Projects for "Major New Drugs Innovation and Development" (grant No. 2019ZX09201001-004-001), the Project Program of National Natural Science Foundation of China (Grant No. 81872757), the Project Program of Natural Science Foundation of Jiangsu Province of China (Grant No. BK20201329), the Fundamental Research Funds for the Central Universities (grant No. 2632018ZD01), Innovation and Entrepreneurship Training Program for Undergraduate (No. 201910316220 and No. 202010316245), the Priority Academic Program Development of Jiangsu Higher Education Institution and Qing Lan Project.

Appendix A. Supplementary material

Supplementary data to this article can be found online at https://doi.org/10.1016/j.bioorg.2021.104736.

References

[1] N. Guttenberger, W. Blankenfeldt, R. Breinbauer, Bioorg. Med. Chem. 25 (2017) 6149.
[2] J. Zhang, X. Li, X. Han, R. Liu, J. Fang, Trends Pharmacol. Sci. 38 (2017) 794.
[3] L. Xie, Z. Luo, Z. Zhao, T. Chen, J. Med. Chem. 60 (2017) 202.
[4] X. Cheng, P. Holenya, S. Can, H. Alborzinia, R. Rubbiani, I. Ott, S. Wölfl, Mol. Cancer 13 (2014) 1.
[5] H. Sies, D.P. Jones, Nat. Rev. Mol. Cell Biol. 21 (2020) 363.
[6] X. Gao, Y. Lu, Y. Xing, Y. Ma, J. Lu, W. Bao, Y. Wang, T. Xi, Microbiol. Res. 167 (2012) 616.
[7] X. Gao, Y. Lu, L. Fang, X. Fang, Y. Xing, S. Gou, T. Xi, Eur. J. Med. Chem. 69 (2013) 1.
[8] J. Gao, M. Chen, X. Tong, H. Zhu, H. Yan, D. Liu, W. Li, S. Qi, D. Xiao, Y. Wang, Y. Lu, F. Jiang, Comb. Chem. High Throughput Screen. 18 (2015) 960.
[9] Y. Lu, Y. Yan, L. Wang, X. Wang, J. Gao, T. Xi, Z. Wang, F. Jiang, Eur. J. Med. Chem. 127 (2017) 928.
[10] Y. Lu, L. Wang, X. Wang, T. Xi, J. Liao, Z. Wang, F. Jiang, Eur. J. Med. Chem. 135 (2017) 125.
[11] M. Zhang, S. Gu, G. Liu, C. Li, H. Xu, Z. Wu, B. Ye, Y. Lu, D. Huang, Z. Wang, F. Jiang, Comb. Chem. High Throughput Screen. 22 (2019) 35.
[12] J. Liao, L. Wang, Z. Wu, Z. Wang, J. Chen, Y. Zhong, F. Jiang, Y. Lu, J. Enzyme Inhib. Med. Chem. 34 (2019) 1158.
[13] J. Chen, Y. Zhang, X. Jie, J. She, G. Dongye, Y. Zhong, Y. Deng, J. Wang, B. Guo, L. Chen, J. Inorg. Biochem. 193 (2019) 112.
[14] S. Busker, W. Qian, M. Haraldsson, B. Espinosa, L. Johansson, S. Attarha, I. Kolosenko, J. Liu, M. Dagnell, D. Grandér, E.S.J. Arnér, K. Pokrovskaja Tamm, B.D. G. Page, Sci. Adv. 6 (2020) eaax7945.
[15] Y. Zhang, J. Zhou, Q. Ye, K. Zeng, J. Pan, L. Chen, Y. Wang, B. Yang, Q. He, J. Gao, S. Zeng, L. Yu, Toxicol. Appl. Pharmacol. 401 (2020) 115079.
[16] J. Zhang, Y. Liu, D. Shi, G. Hu, B. Zhang, X. Li, R. Liu, X. Han, X. Yao, J. Fang, Eur. J. Med. Chem. 140 (2017) 435.
[17] C. Zhuang, W. Zhang, C. Sheng, W. Zhang, C. Xing, Z. Miao, Chem. Rev. 117 (2017) 7762.
[18] M. Decker, Curr. Med. Chem. 18 (2011) 1464.
[19] K. Nepali, S. Sharma, M. Sharma, P.M. Bedi, K.L. Dhar, Eur. J. Med. Chem. 77 (2014) 422.
[20] Shaveta, S. Mishra, P. Singh, Eur. J. Med. Chem. 124 (2016) 500.
[21] A.T. Garrison, Y. Abouelhassan, D. Kallifidas, H. Tan, Y.S. Kim, S. Jin, H. Luesch, R. W. Huigens III, J. Med. Chem. 61 (2018) 3962.
[22] A.A. El Bahnasawy, M.F. El Ahwany, Phosphorus, sulfur, and silicon and the related elements, 182 (2007) 1937.
[23] C. Seillan, H. Brisset, O. Siri, Org. Lett. 10 (2008) 4013.
[24] N.G. Paciaroni, N.V. Borrero, J.R. Rocca, R.W. Huigens III, Res. Rev.: J. Med. Org. Chem. 2 (2015) 67.
[25] T. Liu, J. Zhang, X. Han, J. Xu, Y. Wu, J. Fang, Free Radical Biol. Med. 135 (2019) 216.
[26] M. del P.S. Idelchik, U. Begley, T.J. Begley, J.A. Melendez, Semin. Cancer Biol. 47 (2017) 57.
[27] V.R. Pannala, R.K. Dash, Free Radical Biol. Med. 78 (2015) 42.
[28] K. Hui, Y. Yang, K. Shi, H. Luo, J. Duan, J. An, P. Wu, Y. Ci, L. Shi, C. Xu, Cancer Lett. 354 (2014) 189.
[29] Y. Xiang, W. Ye, C. Huang, B. Lou, J. Zhang, D. Yu, X. Huang, B. Chen, M. Zhou, Biochem. Biophys. Res. Commun. 487 (2017) 820.
[30] G.M. Jose, M. Raghavankutty, G.M. Kurup, Process Biochem. 68 (2018) 197.
[31] M. Bian, R. Fan, S. Zhao, W. Liu, J. Med. Chem. 62 (2019) 7309.
[32] S.A. Ansari, U.R. Pendurthi, L.V.M. Rao, Blood Adv. 1 (2017) 2399.
[33] E.S.J. Arnér, A. Holmgren, Semin. Cancer Biol. 16 (2006) 420.
[34] V. Branco, L. Coppo, S. Solá, J. Lu, C.M.P. Rodrigues, A. Holmgren, C. Carvalho, Redox Biol. 13 (2017) 278.
[35] E.F. Wagner, Á.R. Nebreda, Nat. Rev. Cancer 9 (2009) 537.
[36] A.G. Barata, T.P. Dick, Redox Biol. 28 (2020), 101340.